Science Advances
AAAS

advances.sciencemag.org/cgi/content/full/6/46/eabc1087/DC1

Supplementary Materials for

Adaptive tuning of cell sensory diversity without changes in gene expression

K. Kamino, J. M. Keegstra, J. Long, T. Emonet*, T. S. Shimizu*

*Corresponding author. Email: shimizu@amolf.nl (T.S.S.); thierry.emonet@yale.edu (T.E.)

Published 13 November 2020, *Sci. Adv.* **6**, eabc1087 (2020)
DOI: 10.1126/sciadv.abc1087

This PDF file includes:

The MWC model with response adaptation and cell-to-cell variation

In this study, we utilize the standard model (the MWC model) of the receptor-kinase complex in the *E.coli* chemotaxis pathway (*20, 23, 35-42*). The model is well constrained from population data, but, in this study, we discuss cell-to-cell variability of the model parameters as well. The model assumes that n two-activity-state receptors form a tightly-coupled signaling team switching between active and inactive states together. Studies have shown that the kinase activity of the pathway can be described by a two-state model:

$$a = \frac{1}{1 + e^{f([L],m)}} \qquad \text{(Eq. S1)},$$

where $f([L], m)$ is the free energy of the active state of the coupled receptors relative to the inactive state as a function of the ligand (MeAsp or serine) concentration $[L]$ and the average methylation level of a receptor ($0 < m < 4$). The free energy can be decomposed into two parts describing respectively the contributions from ligand binding to the receptors and the methylation level of the receptors:

$$f([L], m) = f_L([L]) + f_m(m).$$

The ligand dependent free-energy term can be written as:

$$f_L([L]) = n \ln\left(\frac{1 + \frac{[L]}{K_I}}{1 + \frac{[L]}{K_A}}\right) \approx n \ln\left(1 + \frac{[L]}{K_I}\right)$$

where K_I and K_A are respectively the dissociation constants of the receptors in inactive and active states, whose values are experimentally determined as $K_I = 18$ μM and $K_A = 2900$ μM for MeAsp (*14, 20*) and $K_I = 4$ μM and $K_A = 20$ μM for serine (*58*). We hereafter assume $\frac{[L]}{K_A} \ll 1$. The methylation dependent free-energy can be written as

$$f_m(m) = -n\alpha(m - m_0), \qquad \text{(Eq. S2)}$$

where α is the free energy change of a receptor per methylation and m_0 is the methylation level at which two states are equally stable in absence of ligand, whose values are experimentally determined as $\alpha = 2\ k_B T$, $m_0 = 0.5$ (*20*).

At steady states, the kinase activity shows a constant value irrespective of the stimulus level - a property called perfect adaptation – due to the feedback regulation of the methylation level by the methylation/demetylation enzymes. This constrains the functional form of m at steady state as a function of the background stimulus $[L]_0$, $m = m([L]_0)$. Specifically, by equating $a([L] = 0)$ and $a([L] = [L_0])$, we obtain the methylation level in the stimulus level $[L]_0$ at steady state as

$$m([L]_0) \equiv \frac{1}{\alpha}\log\left(1 + \frac{[L]_0}{K_I}\right) + m^*, \quad \text{(Eq. S3)}$$

where $m^* = m([L]_0 = 0)$ is the methylation level in the absence of ligand. Since the timescale of the change of the methylation level ($\sim$ 10 sec) is much larger than that of the change of the ligand-dependent free-energy change ($\ll$ 1 sec), upon a step change of the ligand concentration from $[L]_0$ to $[L]$, only the ligand-dependent free-energy term changes as $f_L([L]_0) \to f_L([L])$, whereas the methylation level stays $m([L]_0)$ until the process of response adaptation begins to take effect. Thus, by plugging Eq. S3 in Eq. S1 and S2, we obtain the kinase activity upon a step stimulus from $[L]_0$ to $[L]$ as

$$a([L]|n, m^*, [L]_0) = \frac{1}{1 + e^{f_L([L]) + f_m(m([L]_0))}}$$

$$= \frac{1}{1 + \exp\left(n\alpha(m_0 - m^*) + n\ln\left(\frac{1 + \frac{[L]}{K_I}}{1 + \frac{[L]_0}{K_I}}\right)\right)}$$

$$= \frac{1}{1 + e^{f(n, m^*, [L]_0, [L])}}.$$

Note the parameters α, m_0 and K_I (and K_A) are biochemical constants, and since they are primarily determined by the protein structures, we assume they are invariant across cells. On the other hand, parameters n and $m^*$are mesoscopic, phenomenological parameters whose values are dependent on many factors such as the abundances of relevant proteins as well as the type of receptors (i.e., Tar or Tsr) to be considered. Thus, we see it as cell-dependent parameters that affect the kinase activity.

The steady-state kinase activity can be given as:

$$a(0|n, m^*, 0) = \frac{1}{1 + e^{n\alpha(m_0 - m^*)}} = a_0(n, m^*).$$

The inhibition constant $K_{1/2}$ for half-maximal response at a background stimulus $[L]_0$ is defined as

$a\left(K_{1/2}\middle|n, m^*, [L]_0\right) = \frac{1}{2}a([L]_0|n, m^*, [L]_0)$.

This gives:

$$K_{1/2}(n, m^*|[L]_0) = K_I\left(\left(e^{-\alpha n(m_0 - m^*)} + 2\right)^{\frac{1}{n}}\left(1 + \frac{[L]_0}{K_I}\right) - 1\right). \quad \text{(Eq. S4)}$$

Two regimes of the MWC model with adaptation and cell-to-cell variation

The inverse sensitivity $K_{1/2}$ of the MWC model with adaptation and cell-to-cell variation in n shows two distinct behavior depending on the background stimulus level $[L]_0$. To see this, we compute the derivative of $\log K_{1/2}$ with respect to n:

$$\frac{\partial \log K_{1/2}(n, m^*|[L]_0)}{\partial n} = \frac{\partial K_{1/2}}{\partial n} / K_{1/2}$$
$$= \frac{-\alpha(m_0 - m^*)\left(1 + \frac{[L]_0}{K_I}\right) e^{-n\alpha(m_0 - m^*)}}{n\left(\left(1 + \frac{[L]_0}{K_I}\right)(e^{-n\alpha(m_0 - m^*)} + 2)^{\frac{1}{n}} - 1\right)(e^{-n\alpha(m_0 - m^*)} + 2)^{1 - \frac{1}{n}}}.$$

According to the theory (*37*), the boundary between the two regimes are set by the methylation level at which the free energy difference between the active and inactive unbound receptors becomes zero, m_0. From Eq. S3, the adapted receptor modification level m is smaller than m_0 when $[L]_0 \ll K_I$, whereas it is larger than $[L]_0 \gg K_I$. In these two limits, we get

$$\frac{\partial \log K_{1/2}(n, m^*|[L]_0)}{\partial n}$$
$$= \begin{cases} \frac{-\alpha(m_0 - m^*)e^{-n\alpha(m_0 - m^*)}}{n} \frac{1}{e^{-n\alpha(m_0 - m^*)} + 2 - (e^{-n\alpha(m_0 - m^*)} + 2)^{1 - \frac{1}{n}}} & ([L]_0 \ll K_I) \\ \frac{-\alpha(m_0 - m^*)e^{-n\alpha(m_0 - m^*)}}{n} \frac{1}{e^{-n\alpha(m_0 - m^*)} + 2} & ([L]_0 \gg K_I) \end{cases}.$$

Note $m_0 - m^* > 0$, and $1 - \frac{1}{n} \lesssim 1$ since n is typically on the order of 10. Thus,

$$\left|\frac{\partial \log K_{1/2}(n, m^*|[L]_0 \ll K_I)}{\partial n}\right| \gg \left|\frac{\partial \log K_{1/2}(n, m^*|[L]_0 \gg K_I)}{\partial n}\right|,$$

i.e., the susceptibility of $K_{1/2}$ to the change of n is strongly dependent on $[L]_0$ and show two regimes (Fig. S10).

Physical origin of the two regimes in the MWC model with response adaptation

Here we discuss a physical interpretation of the mechanism by which the two regimes emerge in the two-state coupled receptor (MWC) model with response adaptation. Following Mello and Tu (*36*), the energy function (Hamiltonian) of the system consisting of coupled n two-state receptors can be written as

$$H = \left(n\left(E_{on} - E_{off}\right) + \epsilon \sum_i \sigma_i \right) s + nE_{off} + \mu \sum_i \sigma_i,$$

where $E_{on}$and E_{off} are respectively the free energies of active and inactive receptors, the ligand occupancy of the i-th receptor is given by σ_i: $\sigma_i = 0, 1$ for vacant and occupied receptor respectively ($i = 1,2, \dots, n$), and the activity of the coupled receptors is either active ($s = 1$) or inactive ($s = 0$). All energies are in units of the thermal energy $k_B T$. The parameters that appears in the energy function can be rewritten using the parameters used above as

$$E_{on} - E_{off} = -\alpha(m([L]_0) - m_0),\ e^{-\epsilon} = \frac{K_I}{K_A},\ e^{-\mu} = \frac{[L]}{K_I},$$

where $[L]_0$ and $[L]$ are background and current attractant concentration respectively.

Note the partition function is:

$$Z = \sum_{all\ states} e^{-H}$$

$$= e^{-nE_{on}}\left(1 + e^{-(\epsilon+\mu)}\right)^N + e^{-nE_{off}}(1 + e^{-\mu})^N.$$

And the kinase activity is given as:

$$a \equiv \langle s \rangle = -Z^{-1}\frac{\partial Z}{\partial(nE_{on})} = \frac{1}{1 + e^{-\alpha n(m([L]_0) - m_0)}\left(\frac{1 + \frac{[L]}{K_I}}{1 + \frac{[L]}{K_A}}\right)^n},$$

which reproduces the expression obtained above (Eq. S1).

We consider the following four states of the system, i.e., either active or inactive, and either no receptor is occupied by ligand or at least one receptor is occupied (i.e., 2 x 2 states):

$$H(s = 1, \sigma_i = 0) = nE_{on},$$

$$H(s = 0, \sigma_i = 0) = nE_{off},$$

$$H(s = 1, \sigma_i \neq 0) = nE_{on} + (\epsilon + \mu)\sum_i \sigma_i,$$

$$H(s = 0, \sigma_i \neq 0) = nE_{off} + \mu \sum_i \sigma_i.$$

The corresponding free energies can be written as

$$F_{A,0} = nE_{on}$$

$$F_{I,0} = nE_{off}$$

$$F_{A,L} = nE_{on} - \log\left(\left(1 + \frac{[L]}{K_A}\right)^n - 1\right)$$

$$F_{I,L} = nE_{off} - \log\left(\left(1 + \frac{[L]}{K_I}\right)^n - 1\right),$$

where the subscripts A and L in F indicate active and inactive respectively, and the subscripts 0 and L indicate the absence and presence of at least one receptor-bound ligand respectively. The fourth equation can be derived by noting:

$$\sum_{\sigma_i} e^{-H(s=0,\sigma_i\neq 0)} = \sum_{\sigma_i} e^{-nE_{off}+\mu\sum_i \sigma_i}$$

$$= e^{-nE_{off}}\left(\sum_{\sigma_i} e^{-\mu\sum_i \sigma_i}\right)$$

$$= e^{-nE_{off}}\left(\binom{n}{1}e^{-\mu} + \binom{n}{2}e^{-2\mu} + \cdots + \binom{n}{n}e^{-n\mu}\right)$$

$$= e^{-nE_{off}}((1 + e^{-\mu})^n - 1)$$

$$= e^{-\left(nE_{on} - \log\left(\left(1+\frac{[L]}{K_A}\right)^n - 1\right)\right)}.$$

And the third equation can be derived in the same way. Using the free energies, the kinase activity can be rewritten as

$$a = \frac{e^{-F_{A,0}} + e^{-F_{A,L}}}{e^{-F_{A,0}} + e^{-F_{I,0}} + e^{-F_{A,L}} + e^{-F_{I,L}}},$$

and thus, the kinase activity, as well as the response sensitivity, is described in terms of the energy balance between the four states.

Using the parameter values obtained from the literature (*14, 20*) and this work, $\alpha = 2\ k_B T$, $m_0 = 0.5$, $K_I = 18$ μM, $K_A = 2900$ μM and $m^* = 0.445$, and the population average of the number of coupled receptors $\langle n \rangle = 8$ the free energy of each state is plotted against the ligand concentration in the case of zero background (Fig. S11a). In this case, because of the low methylation ($m < m_0$), the free energy of the active, ligand-bound state $F_{A,L}$ is significantly larger (i.e., unstable) than others, and hence the kinase activity is approximately given as

$$a \approx \frac{e^{-F_{A,0}}}{e^{-F_{A,0}} + e^{-F_{I,0}} + e^{-F_{I,L}}}.$$

The only stimulus-dependent term is the one corresponding inactive, ligand-bound state (i.e., $e^{-F_{I,L}}$), which is zero at $[L] = 0$, and therefore the inhibition constant $K_{1/2}$ is given by the stimulus level at which the inactive, ligand-bound state is as dominant as other two states. Namely,

$$e^{-F_{A,0}} + e^{-F_{I,0}} \approx e^{-F_{I,L}},$$

which gives

$$K_{1/2} \approx K_I \left(\left(e^{n\alpha(m^* - m_0)} + 2 \right)^{\frac{1}{n}} - 1 \right).$$

On the other hand, when the adapted methylation level m is higher than m_0 due to high background stimulus level ($[L]_0 \gg K_I$), the free-energy of the active state E_{on} get smaller compared with that of inactive state E_{off} (i.e., $E_{on} - E_{off} = -\alpha(m([L]_0) - m_0) < 0$). As a result, the inactive, ligand-free state becomes relatively unstable, and the kinase activity is approximately given as

$$a \approx \frac{e^{-F_{A,0}} + e^{-F_{A,L}}}{e^{-F_{A,0}} + e^{-F_{A,L}} + e^{-F_{I,L}}}.$$

The inhibition constant $K_{1/2}$ is determined by the synergistic effect of the two terms, $e^{-F_{A,L}}$ and $e^{-F_{I,L}}$, which at $[L] = K_{1/2}$ satisfy:

$$\frac{1}{2} \frac{e^{-F_{A,0}} + e^{-F_{A,L_0}}}{e^{-F_{A,0}} + e^{-F_{A,L_0}} + e^{-F_{I,L_0}}} \approx \frac{e^{-F_{A,0}} + e^{-F_{A,L}}}{e^{-F_{A,0}} + e^{-F_{A,L}} + e^{-F_{I,L}}},$$

where, e.g., $e^{-F_{A,L_0}}$ means $e^{-F_{A,L}}$ evaluated at $[L] = [L]_0$. This gives

$$K_{1/2} \approx [L]_0 \left(e^{n\alpha(m^* - m_0)} + 2 \right)^{\frac{1}{n}}.$$

These two expressions for $K_{1/2}$ for the two regimes not only well approximate the absolute values of $K_{1/2}$ (Fig. S11b), but also reproduce the two distinct susceptibility of $K_{1/2}$ to n (Fig. S10). In fact, by differentiating $\log K_{1/2}$ with respect to n we get,

$$\frac{\partial \log K_{1/2}\,([L]_0 \ll K_I)}{\partial n} = \frac{-\alpha(m_0 - m^*)e^{-n\alpha(m_0 - m^*)}}{n} \frac{1}{e^{-n\alpha(m_0 - m^*)} + 2 - \left(e^{-n\alpha(m_0 - m^*)} + 2\right)^{1 - \frac{1}{n}}},$$

for $[L]_0 \ll K_I$, and

$$\frac{\partial \log K_{1/2}\,([L]_0 \gg K_I)}{\partial n} = \frac{-\alpha(m_0 - m^*)e^{-n\alpha(m_0 - m^*)}}{n} \frac{1}{e^{-n\alpha(m_0 - m^*)} + 2},$$

both of which reproduces the results shown above, and hence explains the two regimes of sensitivity diversity.

The above analysis reveals that the emergence of the two regimes in the MWC model with response adaptation can be understood from the shifts in the free-energy balance between the four states: In the

regime 1 (low-background regime), due to the low methylation, the active, ligand-bound state is unstable, and therefore the inhibition constant $K_{1/2}$ is determined by the relative free energy of the inactive, ligand –bound state to two other states. In the regime 2 (high-background regime), on the other hand, due to the relatively high methylation and ligand concentration, the inactive, ligand-unbound state becomes unstable, so $K_{1/2}$ is determined by the relative free energy of the two ligand-bound states to the active, ligand-unbound state.

Relationship between gain and response range for a homogeneous sensory population

We define the response range of a sensory population as $[L]_{0.9}/[L]_{0.1}$, where $[L]_{0.9}$ ($[L]_{0.1}$) is the stimulus level at which the cell with 95th (5th) percentile sensitivity responds with 90% (10%) of maximum amplitude. The response gain of each cell is defined as the Hill coefficient of the Hill function $R = AK^H/([L]^H + K^H)$ fitted to the response curve. Here, we consider a homogenous cell population in zero background whose response curve follows the Hill function. By definition, $[L]_p$ ($p = 0.1$ or 0.9) satisfies

$$R([L] = 0) \times (1 - p) = \frac{AK^H}{[L]_p^H + K^H}.$$

Solving for $[L]_p$, we get

$$[L]_p = \left(\frac{p}{1-p}\right)^{\frac{1}{H}} K.$$

Using this, the response range can be written as

$$\frac{[L]_{0.9}}{[L]_{0.1}} = 9^{\frac{2}{H}},$$

which is plotted in Fig. S13.

A system that transitions from no FCD to FCD upon increased background does not necessarily show the two-regime behavior in the degree of sensitivity diversity

FRET measurements on *E. coli* chemotaxis signaling pathway have revealed that there are two qualitatively different response regimes depending on the background stimulus level (*14*): In a low background-stimulus level, the response properties are strongly dependent on the absolute levels of the background signals (no fold-change detection (FCD) regime, or linear-response regime), whereas in a high background-stimulus level, the response properties are determined by the relative change in the stimulus level and independent from the absolute levels of the background signals (FCD regime, or log-sensing regime). From this background-stimulus behavior, one might suspect that the no FCD-FCD

transition has a direct relationship with the two sensory diversity regimes (Fig. 5). Here, we analyze a network model, and show that a model that exhibits no FCD-FCD regimes does not necessarily show the two sensory diversity regimes.

We consider the following equation, a modified FCD model with an incoherent feedforward loop network topology (*12, 13, 19, 59*)

$$\tau \frac{dx}{dt} = z + \delta - x$$

$$\frac{dy}{dt} = \frac{Kx}{z + \delta + Kx} - y,$$

where $z = z(t)$ is an input signal, x an internal variable, y an output variable, and τ, δ and K are positive parameters. When $\delta = 0$, the model satisfies the sufficient condition for FCD (*18*), but, when $\delta \neq 0$, the FCD condition breaks unless $z \gg \delta$ and the model shows two response regimes below and above $z \approx \delta$ (Fig. S14b). The system shows perfect adaptation because, at steady state at $z = z_0$, the output variable $y = y_0$ is constant:

$$x_0 = z_0 + \delta$$

$$y_0 = \frac{K}{1 + K}.$$

To evaluate the response sensitivity ($1/K_{1/2}$) of the system, we consider the response of the system to a step stimulus, $z_0 \rightarrow z_0 + \Delta z$. Assuming the time-scale separation of the two variables ($\tau \rightarrow \infty$), upon the step stimulus, y changes from y_0 to $y_0 + \Delta y$ (Fig. S14b). This gives:

$$y_0 + \Delta y = \frac{K}{1 + K + \frac{\Delta z}{z_0 + \delta}}$$

$$\Leftrightarrow \Delta y = \frac{K}{1 + K + \frac{\Delta z}{z_0 + \delta}} - y_0$$

$$= \frac{K}{1 + K + \frac{\Delta z}{z_0 + \delta}} - \frac{K}{1 + K}.$$

Maximum response is given by:

$$\Delta y_{max} = \lim_{\Delta z \rightarrow \infty} \Delta y = -\frac{K}{1 + K}.$$

By normalizing the response by the maximum response, we get a normalized response as a function of Δz:

$$f(\Delta z) \equiv \frac{\Delta y}{\Delta y_{max}} = -\frac{1+K}{K}\left(\frac{K}{1+K+\frac{\Delta z}{z_0+\delta}} - \frac{K}{1+K}\right)$$

$$= 1 - \frac{1+K}{1+K+\frac{\Delta z}{z_0+\delta}}.$$

The inhibition constant $K_{1/2}$ satisfies $f\left(K_{1/2} - z_0\right) = 1/2$. Therefore,

$$f\left(K_{1/2} - z_0\right) = 1 - \frac{1+K}{1+K+\frac{K_{1/2}-z_0}{z_0+\delta}} = \frac{1}{2}$$

$$\Leftrightarrow K_{1/2} = (1+K)(z_0+\delta) + z_0$$

To see how the sensitivity distribution behaves, we consider cell-to-cell variation in the parameter K and how it propagates to the distribution of $K_{1/2}$. The expected value and the variance of $K_{1/2}$ are respectively:

$$\langle K_{1/2}\rangle = (z_0+\delta)\langle K\rangle + 2z_0 + \delta$$

$$\langle\left(K_{1/2} - \langle K_{1/2}\rangle\right)^2\rangle = (z_0+\delta)^2\langle(K - \langle K\rangle)^2\rangle.$$

Assuming that K is log-normally distributed, $p_K(K) = \mathrm{Lognormal}(\mu, \sigma)$, the coefficient of variation (CV) of $K_{1/2}$ is:

$$C_V(z_0|p_K(K)) = \frac{\langle\left(K_{1/2} - \langle K_{1/2}\rangle\right)^2\rangle^{1/2}}{\langle K_{1/2}\rangle} = \frac{\left(e^{\sigma^2}-1\right)^{\frac{1}{2}}}{1 + e^{-\left(\mu+\frac{\sigma^2}{2}\right)}\frac{2z_0+\delta}{z_0+\delta}}.$$

This depends only weakly on the background stimulus z_0. In particular, when the condition $\mu + \frac{\sigma^2}{2} \gtrsim 0$ is satisfied, it becomes: $C_V\left(z_0\middle|p_K(K)\right) \sim \left(e^{\sigma^2}-1\right)^{\frac{1}{2}}$, i.e., independent of z_0 (Fig. S14c). Thus, the presence of no FCD-FCD regimes does not entail the presence of the two sensory diversity regimes.

Parameter values used for MeAsp responses

Name	Definision	Value	References and Explanation
K_I	Dissociation constant of inactive Tar for MeAsp	18 μM	Shimizu et al, Lazova et al
K_A	Dissociation constant of active Tar for MeAsp	2900 μM	Shimizu et al, Lazova et al
α	Free energy change per methylation per receptor dimer	2 kT	Shimizu et al, 2010
m_0	Methylation level at which the free energies of two activity states are equal	0.5	Shimizu et al, 2010
m^*	Methylation level of Tar in absence of stimulus	0.4450	This study (Model 1: n-varying model; Fig. 4)
μ_n	Mean of logarithmic values of the effective number of coupled Tar receptors	2.0177	This study (Model 1: n-varying model; Fig. 4)
σ_n	Standard deviation of logarithmic values of the effective number of coupled Tar receptors	0.3869	This study (Model 1: n-varying model; Fig. 4)

Parameter values used for serine responses

K_I	Dissociation constant of inactive Tsr for serine	4 μM	Hansen et al, 2010
K_A	Dissociation constant of active Tsr for serine	20 μM	Hansen et al, 2010
α	Free energy change per methylation per receptor dimer	2 k_BT	Shimizu et al, 2010
m_0	Methylation level at which the free energies of two activity states are equal	0.5	Shimizu et al, 2010
m^*	Methylation level of Tsr in absence of	0.4838	This study (Fig. S5)

	stimulus		
μ_n	Mean of logarithmic values of the effective number of coupled Tsr receptors	3.2322	This study (Fig. S5)
σ_n	Standard deviation of logarithmic values of the effective number of coupled Tsr receptors	0.4174	This study (Fig. S5)

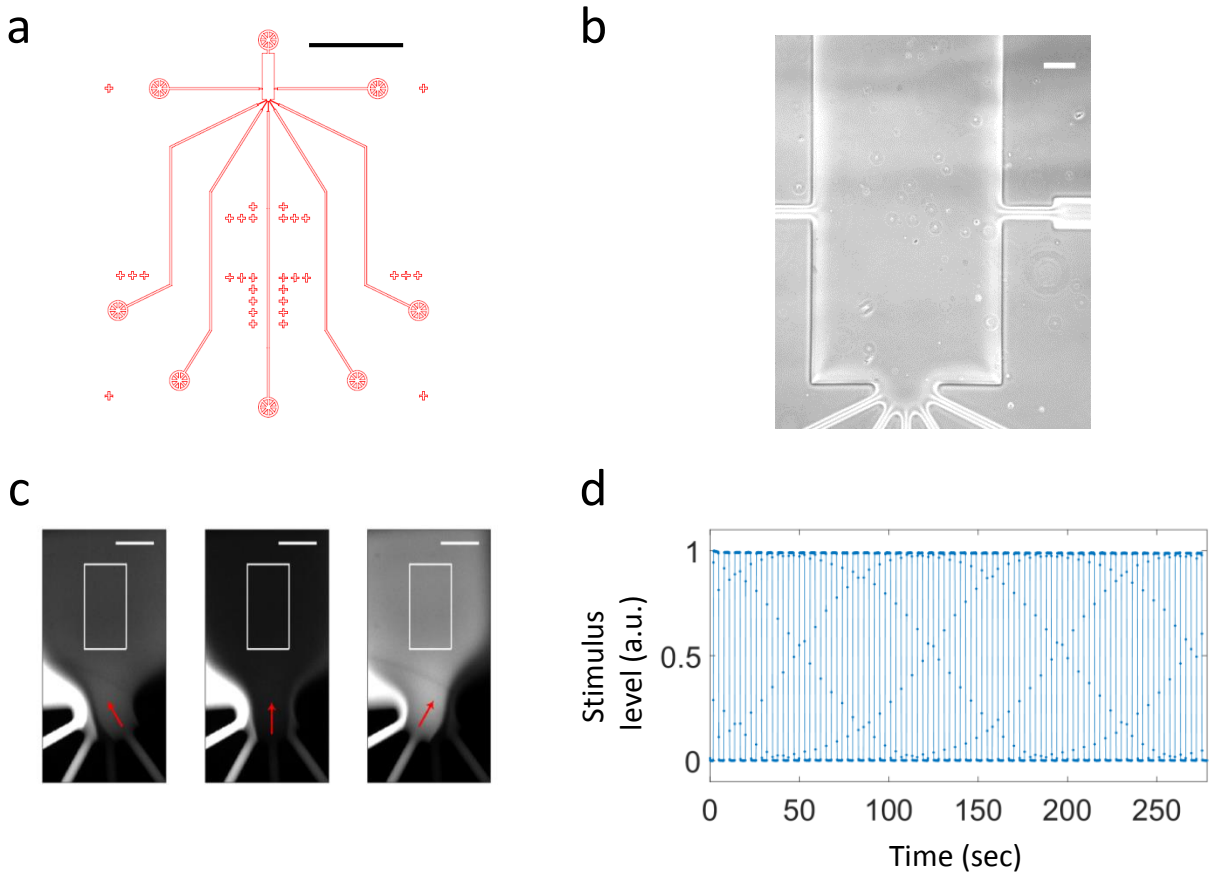

Figure S1. Microfluidic device design and its performance
(a) Design of the microfluidic device. The scale bar is 5 mm. **(b)** Image of the observation chamber. The scale bar is 100 µm. **(c)** Operation of the device. In different images, different channels, which contains different concentrations of fluorescent dye (fluorescein) are pressurized and therefore different solutions are dominant in the main chamber (shown in red arrows). The imaging areas are shown with the rectangle. The scale bar is 100 µm. **(d)** Fluorescent intensity was measured in the observation area in the device while switching between two inlet channels every 3 seconds. The area of region of interest (ROI) over which the signal was averaged was chosen to be the same as the area of ROI for the single-cell FRET measurement. These up and down profiles were overlaid in Fig. 1 (a).

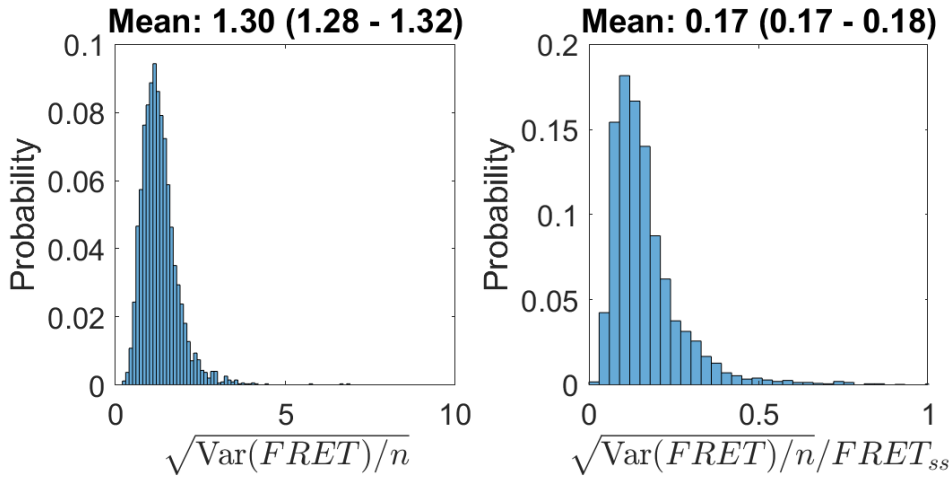

Figure S2. Estimating measurement noise

Histograms of the estimation of measurement noise in our experimental condition quantified by the standard error of the mean in the unit of unnormalized FRET signal (left) and that of normalized FRET signal (right). The standard error of the mean was computed from *n* (= 10) consecutive time points of FRET signal (= 3 sec) of each cell during saturating stimuli, where the fluctuation of the signal is dominated by the measurement noise. 3538 cells are used. The ensemble means and 95% bootstrap confidence intervals are shown.

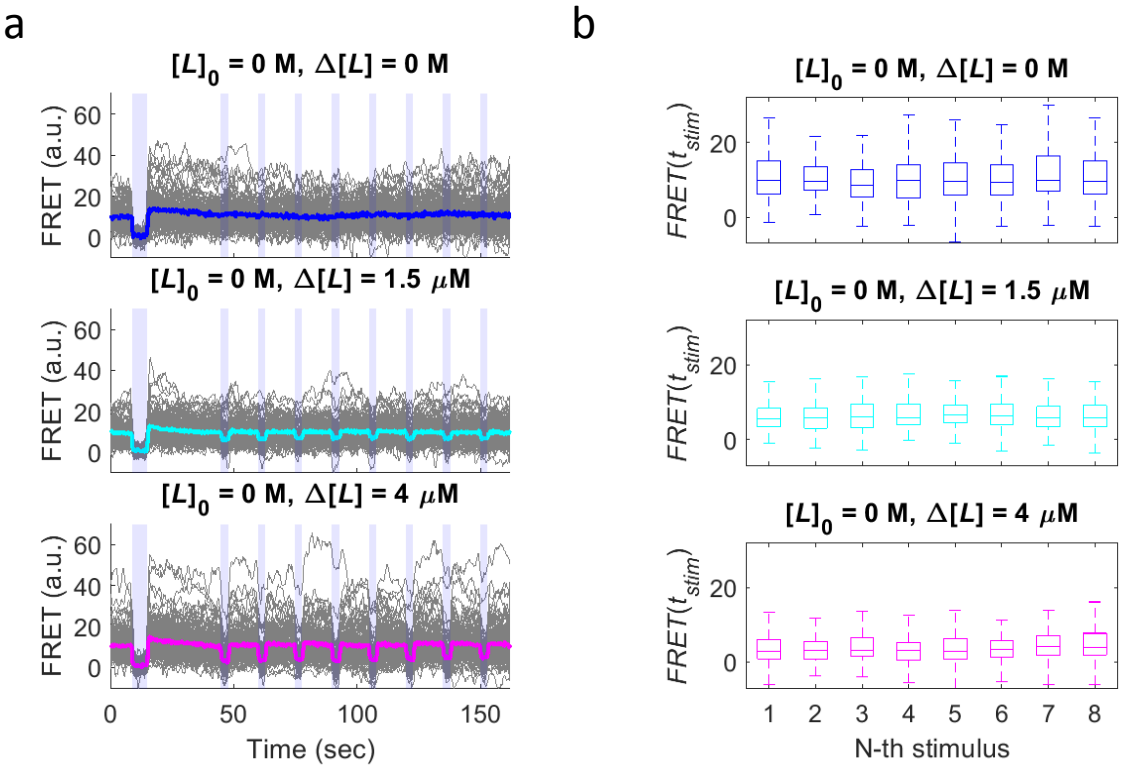

Figure S3. Stationarity of the response distributions within each measurement
(a) FRET time series (not normalized) in three different stimulus conditions in the zero stimulus background ($[L]_0 = 0$ M). Single-cell time series are shown in grey and ensemble averages in colored lines. A saturating stimulus (0.5 mM MeAsp) was applied at about t = 10 seconds, and then eight identical 3-sec stimuli ($\Delta[L]$) of MeAsp were applied. The blue shades indicate the time points in which step stimuli were applied. **(b)** Distributions of $FRET(t_{stim})$ defined as median FRET signal during each 3-second step stimulus. Median and 25th (q_1) and 75th (q_3) percentiles are shown by the boxes . The whiskers extend to the most extreme data points that are not outliers, where outliers are defined as those that are greater than $q_3 + 1.5(q_3 - q_1)$ or less than $q_1 - 1.5(q_3 - q_1)$.

a

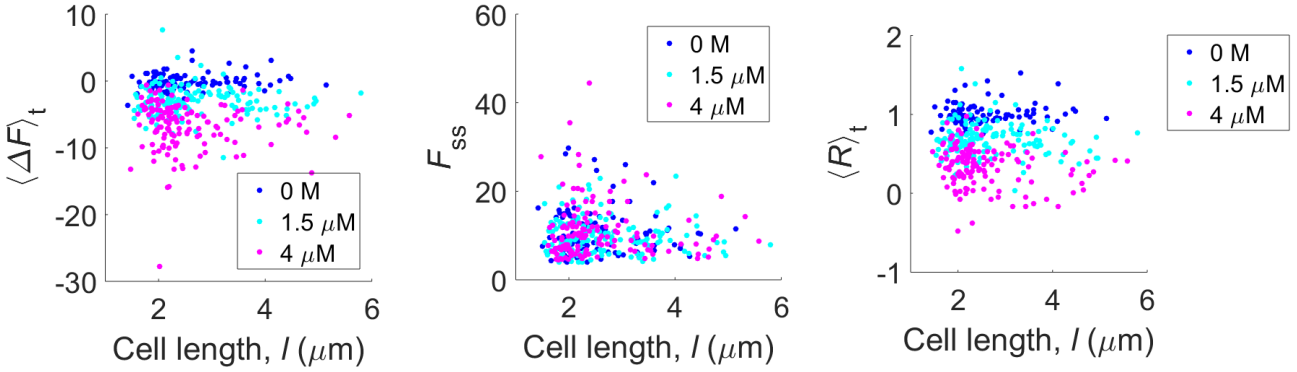

b

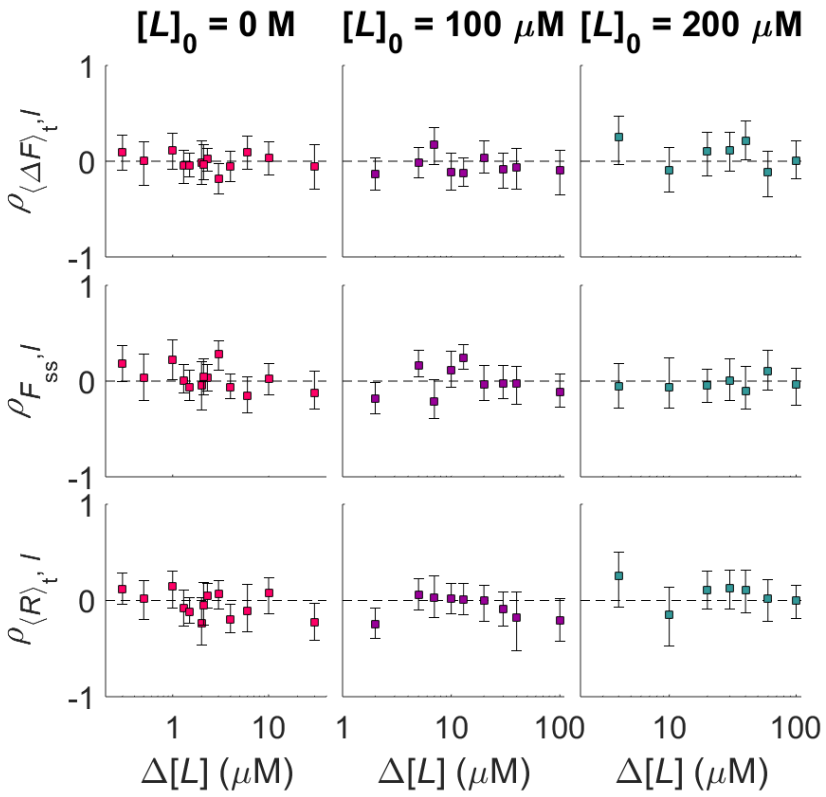

Figure S4. Variation in cell cycle phase does not explain variations in response parameters
(a) Scatter plots of response parameters and cell length l, an indicator of the phase in cell cycle, from three representative stimulus conditions in the zero stimulus background. Intracellular averages of FRET change upon stimulus $\langle \Delta F \rangle_t$, steady-state FRET levels F_{ss}, and intracellular averages of post-stimulus kinase activity $\langle R \rangle_t$ are shown. Each dot comes from single cell. **(b)** Pearson correlation coefficients between $\langle \Delta F \rangle_t$ and l (top panels), between $FRET_{ss}$ and l (middle), and between $\langle R \rangle_t$ and l (bottom) are shown as functions of stimulus levels $\Delta[L]$. Error bars indicate 95% bootstrap confidence intervals.

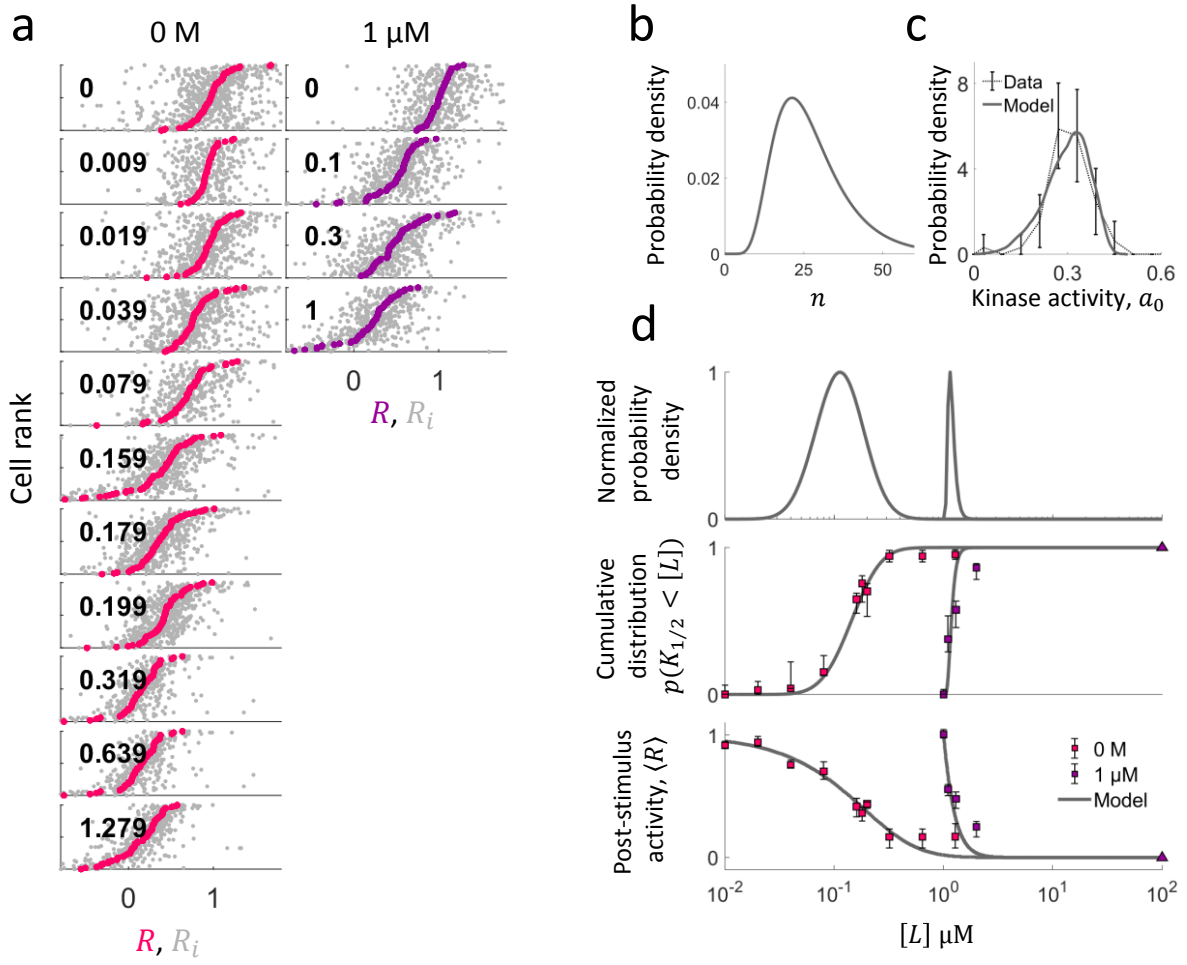

Figure S5. Diversity tuning of sensitivity to serine stimuli

(a) Distributions of post-stimulus kinase activity (grey dots: individual responses R_i, colored dots: median response R). Background concentrations of serine $[L]_0$ and added serine concentration $\Delta[L]$ are shown in μM at the top and in each panel respectively. Cells are sorted by the median response. **(b)** The distribution of the number of coupled receptors n determined by fitting the MWC model with varying n to the data. **(c)** The distribution of steady-state kinase activity a_0. **(d)** The PDF (top) and CDF (middle) of the inverse sensitivity $K_{1/2}$ for serine responses, and population-averaged post-stimulus kinase activity $\langle R \rangle$. Lines are best fits of the MWC model with varying n. The concentration of saturating stimulus used for both 0 M and 1 μM data is indicated by the triangle.

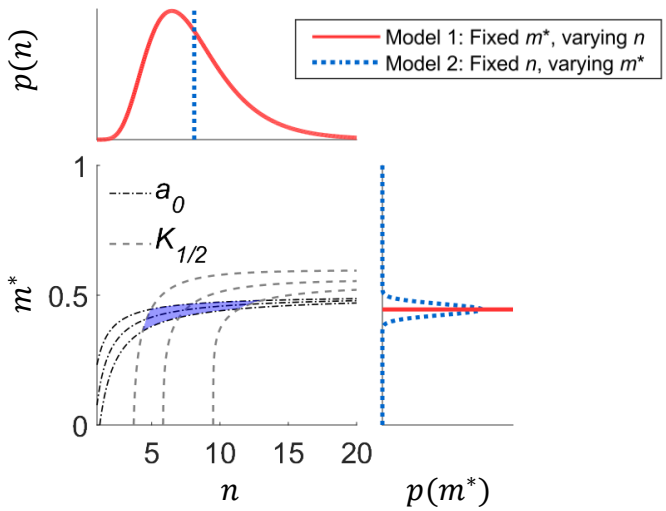

Figure S6. The distributions of the effective number of coupled receptors n and the methylation level in absence of stimulus m^*

The distribution of n (top) and m^*(right) extracted by fitting the MWC models (Fig. 4) to MeAsp response data are shown. Bottom left: The set of (n, m^*) of the MWC model that gives experimentally-determined mean and standard deviation of the distribution of the steady-state kinase activity a_0 and the logarithm of inverse sensitivity $\log(K_{1/2})$ (at $[L]_0 = 0$ M) are shown by the dashed lines. The intersection (blue shade) is wide in n and narrow in m^*, consistent with the parameter distributions of Model 1 (red), which explained the data better than Model 2 (blue) (Fig. 4).

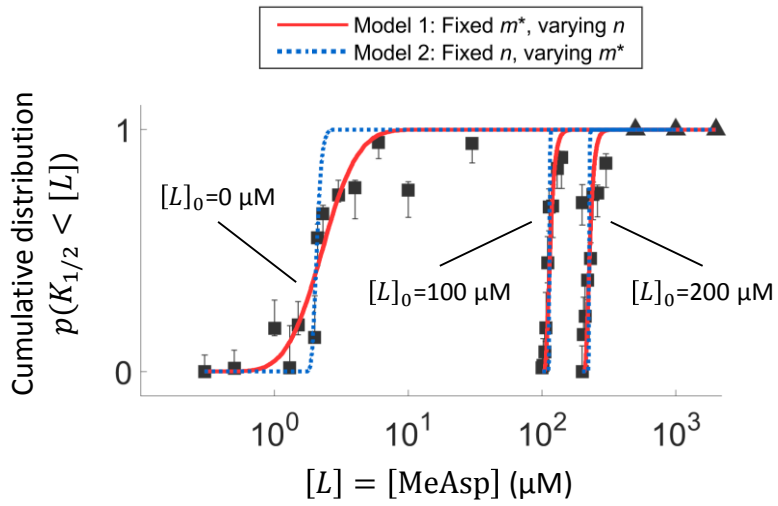

Figure S7. Fits of two limiting cases of the MWC model to data for cumulative distribution of $K_{1/2}$
Fits to data for cumulative distributions of $K_{1/2}$ for the two limiting cases for parameter variation in the MWC model (Model 1 and Model 2, see main text and Fig. 4). The probability density functions shown in Fig. 4e correspond to derivatives of the cumulative distribution fits (Model1: red line, Model2: blue line) shown here. The concentrations of stimuli used for saturating responses are indicated by the triangles.

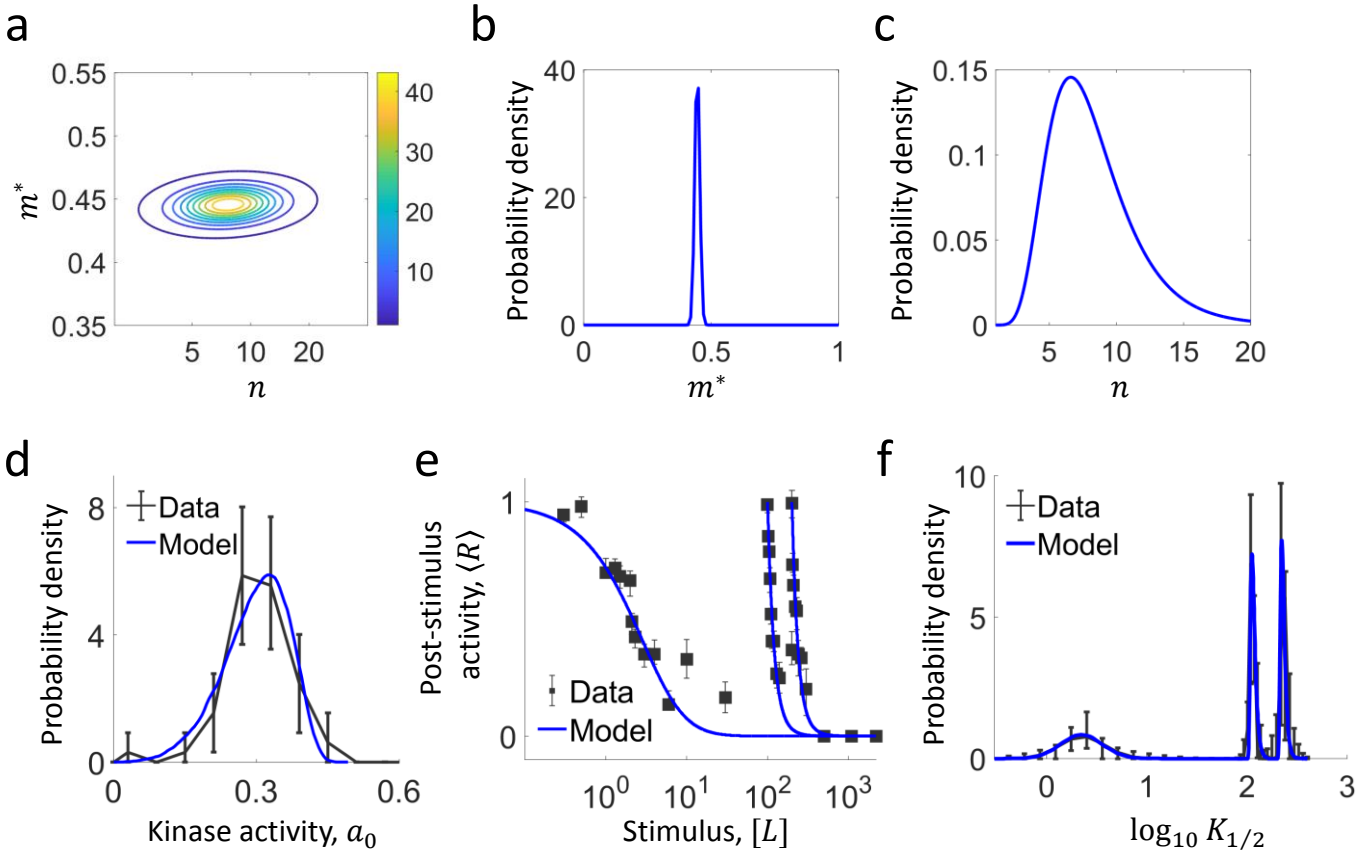

Figure S8. The behavior of the MWC model with two parameters n and m^* varied across cells
(a) The joint distribution of n and m^* obtained by fitting the prediction of the MWC model to the data assuming a 2D Gaussian distribution for m^* and $\log n$. **(b-c)** Marginal distributions of m^* (b) and n (c). **(d-f)** Steady-sate kinase activity a_0 (d), population-averaged post-stimulus activity $\langle R \rangle$ upon MeAsp step stimuli (e), and pdf of $\log K_{1/2}$(f) to MeAsp stimuli are compared with predictions from the MWC model.

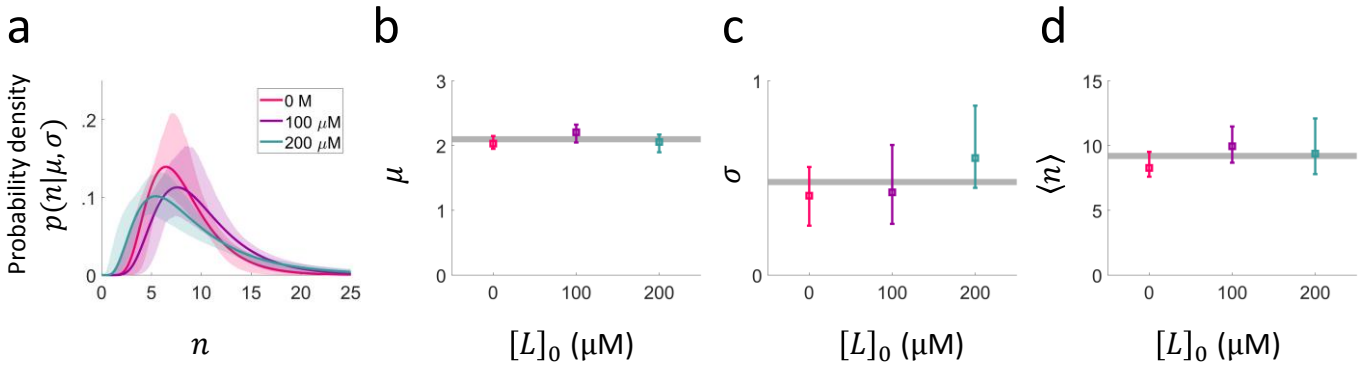

Figure S9. Distributions of cooperativity $p(n)$ from fits at different background $[L]_0$
(a) The distribution of $p(n)$ estimated by maximum-likelihood fitting of Model 1 (defined in Figure 4) to the data of the steady-state distribution of the kinase activity $p(a_0)$, population-averaged dose response $\langle R([L]|[L]_0))\rangle$, and the cumulative distribution of $K_{1/2}$ $p(K_{1/2} < [L]|[L]_0)$, at three different backgrounds $[L]_0 = \{0,100,200\}$ μM MeAsp (Figure 4). $p(n)$ was assumed to be a log-normal distribution parameterized by μ and σ, and the parameters were allowed to vary in different backgrounds (see Methods for detail). 95% confidence intervals are shown by the colored shade. **(b-d)** Parameters μ (b), σ (c), and mean value $\langle n \rangle$ of the fitted log-normal distributions shown in (a), plotted against the corresponding background concentration $[L]_0$. The error bars are 95% confidence interval obtained by Metropolis-Hastings sampling of the likelihood function (see Methods). Neither the fitted parameters nor the mean value $\langle n \rangle$ demonstrate a significant dependence on background.

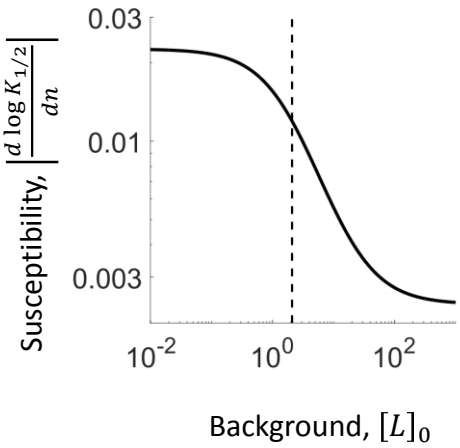

Figure S10. Two regimes of the susceptibility of $K_{1/2}$ to changes in n for MWC model with response adaptation

Susceptibility of $K_{1/2}$ to changes in n as a function of background stimulus level $[L]_0$. The vertical line indicates the crossover background level between the two diversity regimes $[L]_0^* = K_I\left(e^{\alpha(m_0 - m^*)} - 1\right) \approx 2.1$ μM. See SI for the analytical expression of the curve.

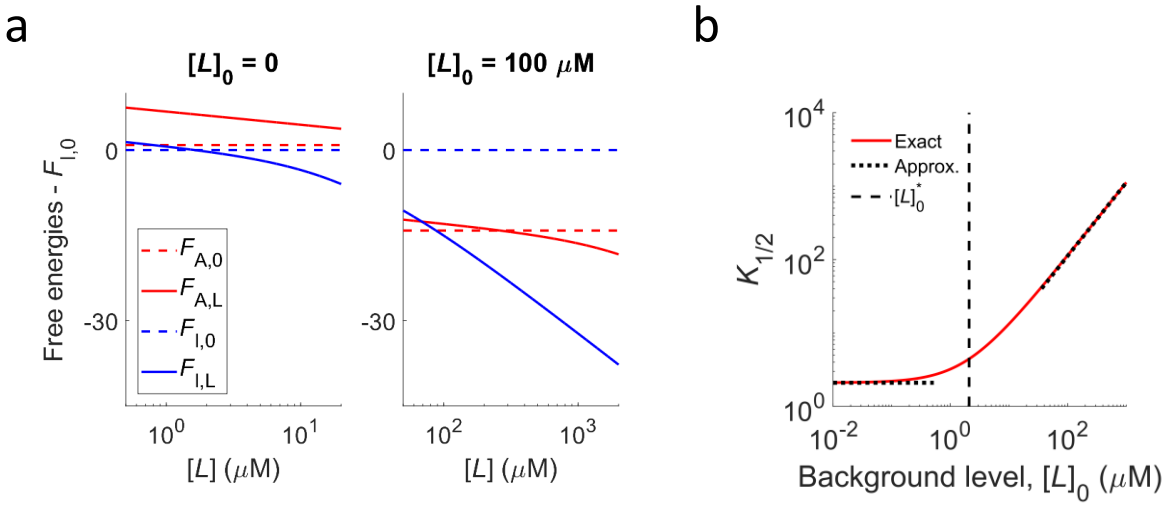

Figure S11. Physical origin of the two-regime behavior in the MWC model with adaptation
(a) Free energies of the four states (active, ligand-unbound $F_{A,0}$; active, ligand-bound $F_{A,L}$; inactive ligand-unbound $F_{I,0}$; inactive ligand-bound $F_{I,L}$) in two different background conditions (see SI Text). **(b)** Exact solution of the inhibition constant $K_{1/2}$ as a function of the background-stimulus level $[L]_0$ and its approximated solution obtained from the energetic consideration (see SI Text).

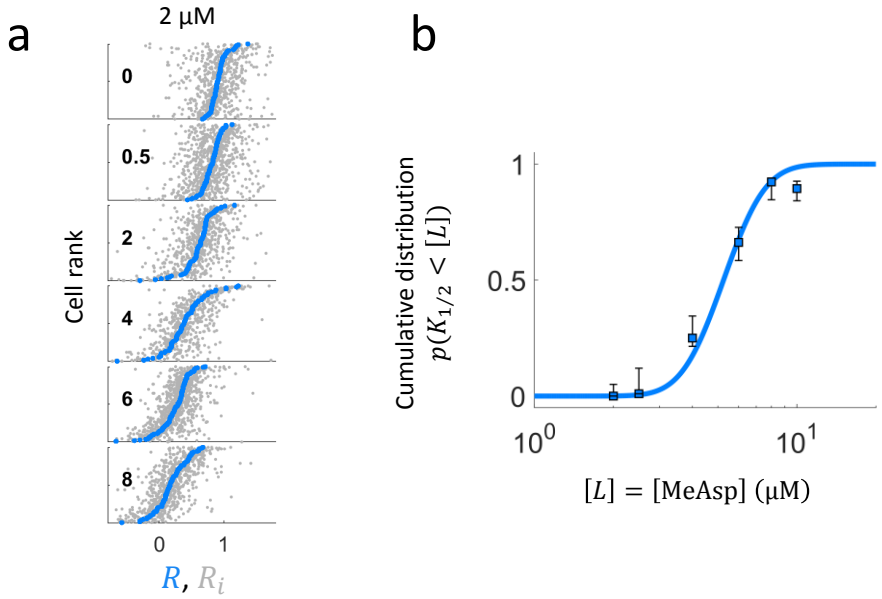

Figure S12. Sensory diversity at a crossover point between the two diversity regimes
(a) Distributions of post-stimulus kinase activity (grey dots: individual responses R_i, colored dots: median response R). Background concentration is $[L]_0 = 2$ μM MeAsp, and added MeAsp concentrations $\Delta[L]$ are shown in μM in each panel. Cells are sorted by the median response (colored dot). **(b)** CDF of the inverse sensitivity $K_{1/2}$ at 2 μM MeAsp background. The error bars represent 95% bootstrap confidence intervals. The curve is the log-normal distribution fitted to the data.

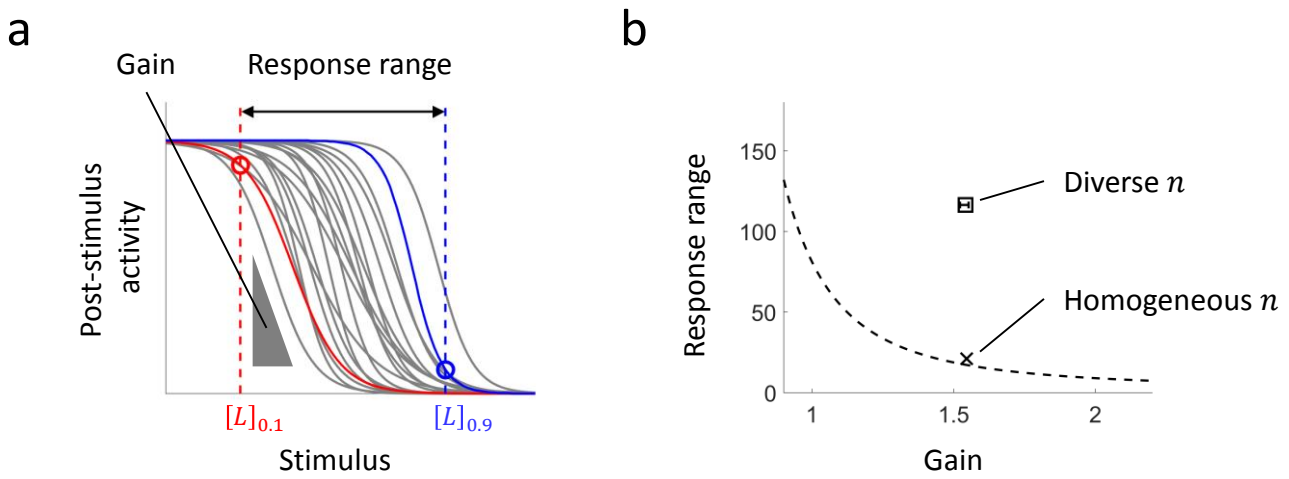

Figure S13. Diverse sensory populations outperform homogeneous populations
(a) The response range of a population is defined as $[L]_{0.9}/[L]_{0.1}$, where $[L]_{0.9}$ ($[L]_{0.1}$) is the stimulus level at which the cell with 95th (5th) percentile sensitivity responds with 90% (10%) of maximum amplitude. The response gain of each cell is defined as the Hill coefficient of the Hill function $R = K^H/([L]^H + K^H)$ fitted to the response curve. **(b)** Performance comparison between the diverse population and homogeneous populations. Diverse n: A collection of the MWC model whose distribution of the number of coupled receptors n follows the experimentally determined one (Model1 in Fig. 4). Homogenous n: A MWC model whose n is set to the average of the diverse population. Any homogenous population with a sigmoidal stimulus-response curve is confined in the points on the dashed line ($y = 9^{2/x}$; See SI)

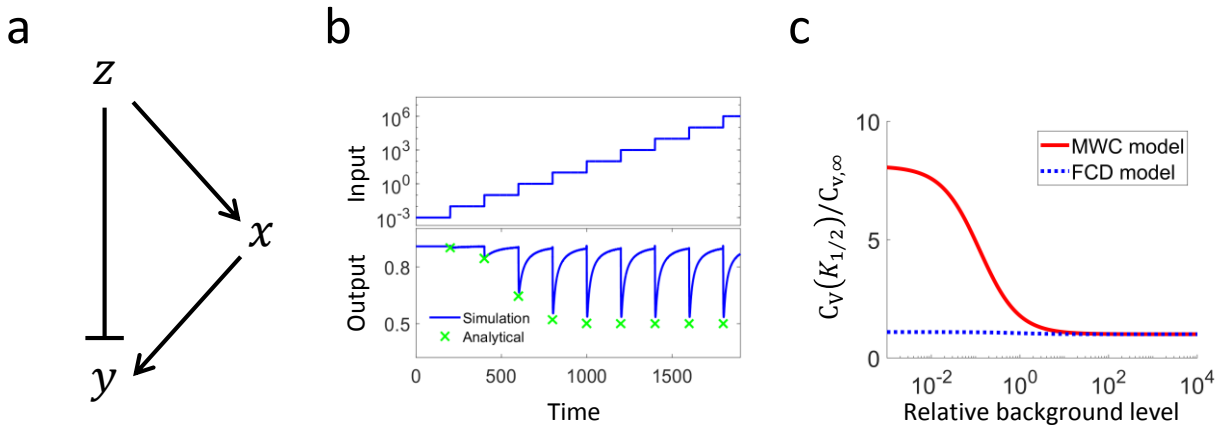

Figure S14. A network model that exhibits linear-response/FCD transition does not necessarily show two distinct sensitivity-diversity regimes

(a) The network topology of the model (SI). **(b)** Successive step stimuli (z) with identical fold change reveal the presence of linear-response regime and fold-change detection (FCD) regime. Peak responses estimated by an analytical calculation is shown by the green symbol. Parameter values used were $K = 10, \tau = 100$, and $\delta = 0.1$. **(c)** The coefficient of variation (CV: C_V) of the inhibition constant $K_{1/2}$ normalized by the CV at infinitely large background stimulus level ($C_{V,\infty}$). Background stimulus (X-axis) was normalized by the parameter that dictates the boundary between linear-response/FCD regimes (K_I for the MWC model and δ for the FCD model). For the FCD model, the parameter K is log-normally distributed $p(K|\mu, \sigma)$, and μ and σ are chosen such that the mean and variance of $p(K)$ are both 10.